

# Supplementary Information for “Ab initio prediction of the polymorph phase diagram for crystalline methanol”

Ctirad Červinka<sup>\*,†</sup> and Gregory J. O. Beran<sup>\*,‡</sup>

*Department of Physical Chemistry, University of Chemistry and Technology Prague, Technická 5, CZ-166 28 Prague 6, Czech Republic, and Department of Chemistry, University of California, Riverside, California 92521 USA*

E-mail: cervinkc@vscht.cz; gregory.beran@ucr.edu

## Contents

<b>S1 Experimental phase diagram and its uncertainty</b>	<b>2</b>
<b>S2 Sample <math>E(V)</math> and <math>A_{vib}</math> data</b>	<b>3</b>
<b>S3 Hartree-Fock vs. AMOEBA many-body treatment</b>	<b>4</b>
<b>S4 Predicted crystal structures</b>	<b>7</b>
S4.1 Comparisons with experiment . . . . .	7
S4.2 Disorder in the $\beta$ phase . . . . .	7
<b>S5 Sensitivity analysis for the predicted phase diagram</b>	<b>9</b>
S5.1 Harmonic versus quasi-harmonic approximation . . . . .	9
S5.2 Impact of electron-electron correlation treatment . . . . .	11
S5.3 Impact of electronic energy well steepness . . . . .	12
S5.4 Impact of phonon frequency scaling . . . . .	13
S5.5 Sensitivity analysis summary . . . . .	16

---

\*To whom correspondence should be addressed

<sup>†</sup>Department of Physical Chemistry, University of Chemistry and Technology Prague, Technická 5, CZ-166 28 Prague 6, Czech Republic

<sup>‡</sup>Department of Chemistry, University of California, Riverside, California 92521 USA

## S1 Experimental phase diagram and its uncertainty

*Ab initio* phase boundaries are difficult to predict reliably, but experimental measurements of the phase coexistence curves can also be difficult, and considerable uncertainty in the experimental boundaries is common. Three experimental studies have reported the methanol  $\alpha$ - $\beta$  phase boundary at various pressures.<sup>1-3</sup> Figure S1 plots this boundary along with a conservative estimate of its uncertainty. On the basis of the scatter of experimental data points, we estimate the uncertainty in temperature of phase transition to be  $\pm 5\%$  for data from Ref 2 and  $\pm 7\%$  from Ref 3. Moreover, the results obtained from different experimental techniques (ultrasonic acoustic measurements<sup>2</sup> and dielectric spectroscopy<sup>3</sup>) differ appreciably. For comparison with the calculations, data from Ref 2 for the low pressure region and selected data from the high-pressure region of Ref 3 were combined and smoothed.

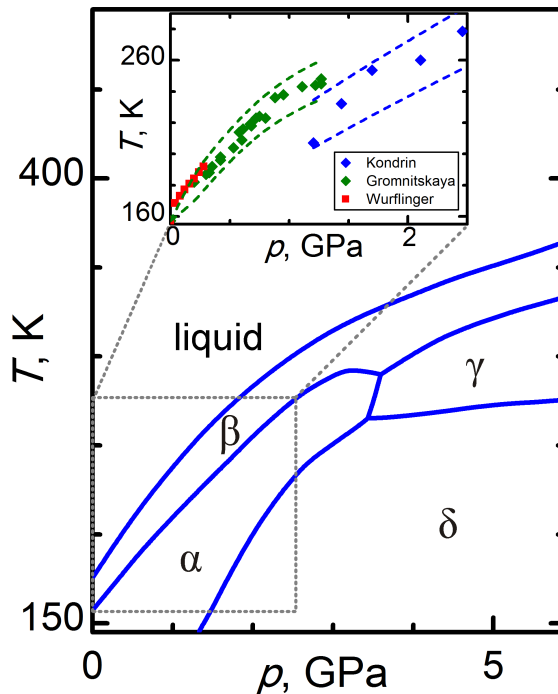


**Figure S1:** Comparison of the  $\alpha$ - $\beta$  phase boundaries from different experimental studies. Dotted lines in inset indicate the estimated uncertainty in the experimental data.

## S2 Sample $E(V)$ and $A_{vib}$ data

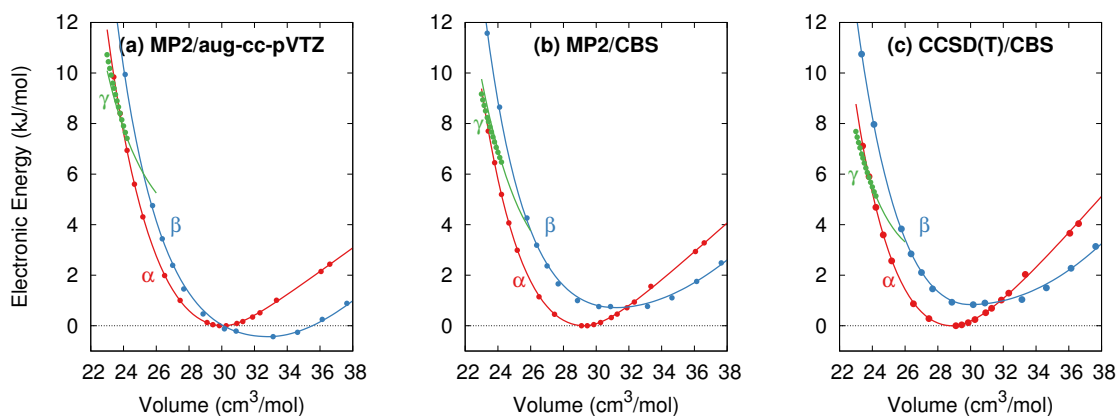


**Figure S2:** Electronic energy versus volume  $E(V)$  for the  $\alpha$  and  $\beta$  polymorphs at the HMBI (a) MP2/aug-cc-pVTZ, (b) MP2/CBS limit, and (c) CCSD(T)/CBS limit, all with periodic HF/pob-TZVP many-body contributions. Geometries were optimized at the MP2 + AMOEBA level of theory.

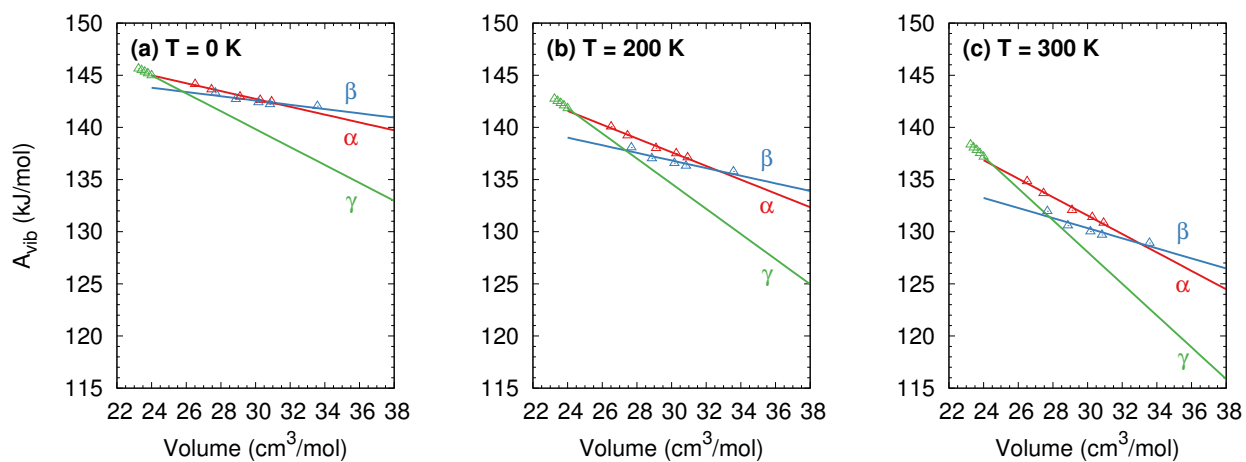


**Figure S3:** Helmholtz vibrational free energy contributions for the  $\alpha$ ,  $\beta$ , and  $\gamma$  phases at three representative temperatures, computed at the MP2 + AMOEBA level of theory.

### S3 Hartree-Fock vs. AMOEBA many-body treatment

We recently reported<sup>4</sup> prediction of structural and thermodynamic properties of  $\alpha$  methanol using the same general approach as the current work, except the AMOEBA force field was always used for the many-body contribution in HMBI. In that work, we considered using geometries from either HMBI MP2/aug-cc-pVTZ + AMOEBA or plane wave PBE-D3 for subsequent HMBI CCSD(T)/CBS + AMOEBA single-point energies. Despite evidence that MP2 provided a better description of methanol-methanol interactions and that the MP2-optimized structures were closer to what one would obtain in a CCSD(T) structure optimization, property predictions based on the PBE-D3 geometries often agreed better with experiment.<sup>4</sup>

Since then, we observed that AMOEBA predicts a many-body contribution in crystalline methanol that is up to 4.5 kJ/mol larger than the one from periodic Hartree-Fock (HF), suggesting that AMOEBA may be overestimating the polarization energy. Therefore, in the final single-point energies in the current work, the AMOEBA many-body contribution was replaced by one calculated from periodic Hartree-Fock (HF) in the pob-TZVP basis<sup>5</sup> (a version of def2-TZVP adapted for crystalline systems). This basis set is computationally affordable, converges well in periodic HF (it does not contain diffuse functions which can cause numerical problems), and produces many-body interaction energies that are fairly well converged with respect to basis set incompleteness. Using periodic HF for the long-range 2-body and the many-body interactions makes HMBI equivalent to the method of increments.<sup>6,7</sup>

The  $E(V)$  curves from the two different many-body treatments are compared in Figure S4. Not only do the crystals become less bound, but the periodic HF many-body contribution reverses the stability of the  $\alpha$  and  $\beta$  forms. Whereas the quasi-harmonic CCSD(T)/CBS + AMOEBA many-body model predicts the  $\beta$  form to be preferred over all temperatures at atmospheric pressure, the results with periodic HF correctly predict that the  $\alpha$  form is the low-temperature form. Interestingly, the HF refinement does lead to a somewhat broader well for the  $\beta$   $E(V)$  curve that is also observed for MP2 (Figure S2), which in turn facilitates thermal expansion of that form. That translates to an overly large molar volume increase at the  $\alpha$ - $\beta$  phase transition: the calculations predict a molar volume increase of 2.07 cm<sup>3</sup>/mol versus 0.49<sup>8</sup> or 0.66<sup>1</sup> cm<sup>3</sup>/mol experimentally. We hypothesize that this shape is an artifact of refining the geometries with AMOEBA many-body terms instead of HF ones.

Repeating several of the  $\alpha$  methanol property predictions with the periodic HF many-body contributions, we find improvement over the earlier predictions relative to experiment and clear superiority for the MP2 geometries over the PBE-D3 ones. As shown in Table S1, using periodic HF instead of AMOEBA for the many-body terms reduces the error in the predicted  $\Delta H_{sub}(0K)$  from 1.9 kJ/mol to 0.7 kJ/mol when using MP2 geometries (*cf* 2.7–2.9 kJ/mol errors from the PBE-D3 geometries).<sup>\*</sup> Periodic HF many-body contributions lead to considerably improved predictions for the molar volume and thermal expansion

---

<sup>\*</sup>For further comparison, a very early study which used periodic HF plus small-basis MP2 corrections predicted a lattice energy of -63 kJ/mol,<sup>9</sup> while a more recent one with point-charge embedding plus a handful of key three-body corrections obtained a lattice energy for  $\alpha$  methanol of 53.78 kJ/mol.<sup>10</sup> compared to the 51.33 kJ/mol (from Table 1 in the main paper) obtained with the periodic HF treatment here. Clearly the specific treatment of many-body effects matters in methanol when striving for sub-kJ/mol accuracy.

(Figure S5). Accordingly, all other calculations reported here employ MP2 + AMOEBA geometries/phonons (for computational affordability) and then MP2 or CCSD(T) + periodic HF single-point energies.

As a side note: although the AMOEBA force field includes van der Waals parameters which were fitted against experimental data,<sup>11</sup> their contributions to the overall results here are negligible. For the  $\alpha$  form, for instance, the long-range van der Waals term amounts to less than 5% of the AMOEBA contribution, or less than 1% of the overall lattice energy. The crystal energetics are dominated by the *ab initio* MP2 and CCSD(T) energies and the AMOEBA electrostatics and polarization terms whose parameters are derived from electronic structure theory, without any specific fitting to experimental data on methanol.

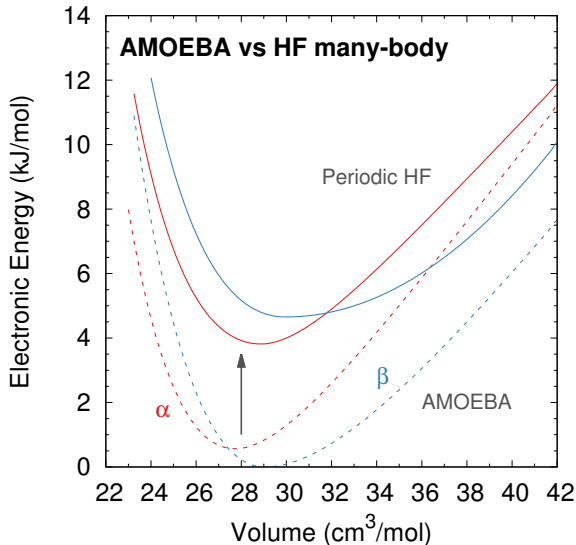


**Figure S4:** Switching the HMBI many-body treatment paired with CCSD(T)/CBS monomers and dimers from AMOEBA (dotted lines) to periodic HF/pob-TZVP (solid lines) decreases the overall binding of the methanol polymorphs by up to 4.5 kJ/mol and reverses the relative stability ordering of the  $\alpha$  and  $\beta$  forms. The periodic HF many-body case reproduces the experimental result that  $\alpha$  is a low-temperature polymorph, while  $\beta$  is the high-temperature form.

**Table S1:** Comparison of experimental and predicted quasi-harmonic sublimation enthalpies  $\Delta H_{sub}(0K)$  for  $\alpha$  methanol (kJ/mol). The calculations employ extrapolated CCSD(T)/CBS 1+2-body contributions plus many-body contributions computed at either the AMOEBA or periodic HF/pob-TZVP level of theory.

Source	MP2/aTZ geometry	PBE-D3 geometry
CCSD(T) + AMOEBA (Ref 4)	47.6	43.0
CCSD(T) + periodic HF (this work)	45.0	42.8
Experiment (Ref 12)	45.7 $\pm$ 0.3	

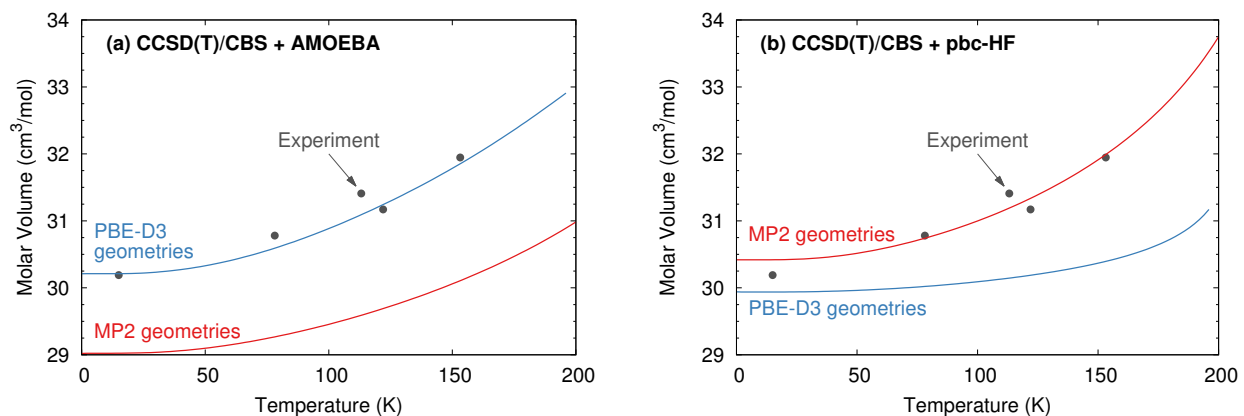


**Figure S5:** Comparison of experimental and predicted molar volumes for  $\alpha$  methanol at ambient pressure with (a) AMOEBA or (b) periodic HF many-body contributions. Plane wave PBE-D3 and HMBI MP2/aug-cc-pVTZ geometries were taken from Ref 4.

## S4 Predicted crystal structures

### S4.1 Comparisons with experiment

To compare the predicted and experimental crystal structures, optimal volumes for the experimental temperature and pressure were determined from the quasi-harmonic CCSD(T)/CBS + periodic HF/pob-TZVP model. Individual lattice constants and fractional coordinates were then obtained via interpolation of the MP2 + AMOEBA geometries (i.e. the structures used to construct the  $E(V)$  curves) to the predicted volume. Figure S6 overlays the predicted and experimental crystal structures for the  $\alpha$ ,  $\beta$ , and  $\gamma$  phases. Lattice parameters are compared in Table 1 of the main paper. Note that the experimental  $\gamma$  structure omits hydrogen atoms, and those were added here.

Interestingly, unconstrained geometry optimization of the experimentally determined  $\gamma$  structure at ambient pressure using HMBI MP2/aug-cc-pVDZ + AMOEBA yields a considerably altered structure that differs from the experimental  $\gamma$  structure in cell volume, cell parameters, and packing motif. To optimize the  $\gamma$  polymorph, an external pressure constraint is required, represented either as a fixed-volume optimization or through minimizing the total enthalpy per cell under the pressure instead of its total energy. Applying an external pressure of 3–5 GPa led to an optimized structure which retains the structural motif of the  $\gamma$  polymorphs and exhibits all real vibrational frequencies. The resulting structures were found to be thermodynamically stable in terms of the Gibbs free energy at low temperatures and high pressures at the CCSD(T)/CBS level of theory, as discussed in Figure 6 of the main paper.

### S4.2 Disorder in the $\beta$ phase

To investigate the nature of the disorder of the  $\beta$  polymorph, we performed multiple unit-cell optimizations of the two  $\beta$  structures: i) with disorder averaged out with all carbon and oxygen atoms in a planar arrangement (as in all of the other results presented here); and ii) with the oxygen atoms distorted from the carbon planes to mimic the limiting positions of the disorder for the experimental crystal structure METHOL05. Unit cell parameters were held fixed during the optimizations, and only the atomic positions were allowed to vary. We compared HMBI MP2/aug-cc-pVDZ + AMOEBA and periodic PBE-D3(BJ)/PAW using VASP (see Ref 4 for discussion of the DFT computational parameters).

MP2 predicts the averaged structure to be more stable than the distorted ones by about 1.5 kJ/mol, which supports the hypothesis about the dynamical disorder and justifies the averaging procedure used for the disorder throughout this paper. Interestingly, however, the periodic DFT calculations favor the distorted structures by 0.3 kJ/mol over the averaged one, suggesting a double-well potential that might point toward a static orientational disorder picture. Because the MP2+AMOEBA geometries overall yield thermodynamic properties in better agreement with experiment, we conclude that the dynamic disorder is the more probable option. This suggests that the  $\beta$  phase disorder should probably be modeled using an anharmonic treatment of the relevant degree(s) of freedom rather than by adding a configurational entropy term.

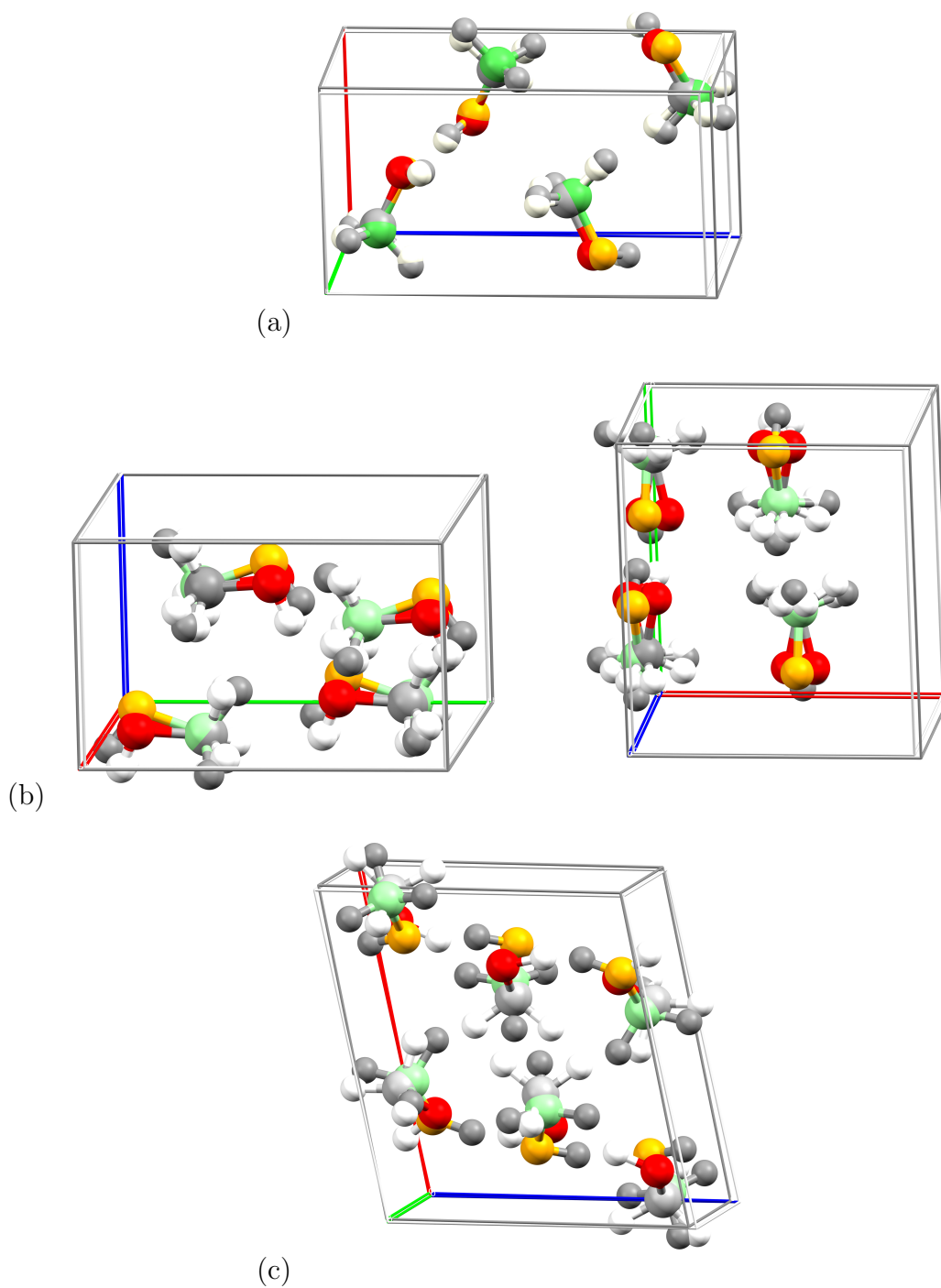


**Figure S6:** Overlays between predicted and experimental structures crystal for (a)  $\alpha$  at 122 K and ambient pressure (RefCode METHOL04), (b)  $\beta$  at 160 K and ambient pressure (METHOL05), and (c)  $\gamma$  methanol at room temperature and 4.0 GPa (METHOL03). Expt: O=red, C=gray, H=white. Pred: O=gold, C=green, H=gray.

## S5 Sensitivity analysis for the predicted phase diagram

The predicted phase diagram derives from a complex interplay of the electronic structure method and phonon treatment. To disentangle how some of these factors impact the predicted phase diagram, the sensitivity of the predicted phase boundaries to several different model features was investigated, as described in the following sections. Most of the analysis centers on the  $\alpha$ - $\beta$  coexistence curve, which exhibits clear pressure and temperature dependence and is sensitive to small perturbations in the models. Unless otherwise stated, results presented here are based on the CCSD(T)/CBS + periodic HF single point energies combined with geometries and phonons computed at the MP2 + AMOEBA level.

### S5.1 Harmonic versus quasi-harmonic approximation

One might simplify the computational model by using harmonic instead of quasi-harmonic estimates for the phonon contributions. Harmonic free energy estimates are often used in crystal structure prediction<sup>13</sup> and polymorph discrimination,<sup>14</sup> for example. A recent computational survey by Nyman and Day found that thermal expansion typically alters relative polymorph stabilities by only a fraction of a kJ/mol, and never more than 2 kJ/mol.<sup>15</sup> Indeed, the harmonic and quasi-harmonic 0 K sublimation enthalpies in Table 1 in the main paper differ by only 0.3 kJ/mol. Nevertheless, given the small energy differences involved in phase diagram predictions, even small changes can have an appreciable impact.

To investigate the impact of the quasi-harmonic treatment here, we recomputed the phase diagram under a harmonic approximation in which the lattice energy, cell volume, and phonon frequencies were assumed to be independent of temperature and pressure.<sup>†</sup> Accordingly, temperature enters the Gibbs free energy  $G(T, P)$  only through the Helmholtz vibrational free energy  $A_{vib}(T)$ , while pressure enters via the  $pV$  term.

Figure S7 compares the resulting phase diagram against the quasi-harmonic one. The harmonic phase diagram completely transforms the regions of phase stability. The  $\alpha$ - $\beta$  coexistence curve now rises too steeply, while the  $\alpha$ - $\gamma$  coexistence shifts to higher pressures. More significantly, the  $\alpha$ - $\beta$ - $\gamma$  triple point disappears. The  $\beta$ - $\gamma$  coexistence curve (indicated as the dotted blue line) would occur in the region where the  $\alpha$  form is the preferred polymorph. Quasi-harmonic thermal expansion clearly plays a significant role in the successful phase diagram prediction.

---

<sup>†</sup>More elaborate harmonic models might recompute the crystal cell volume and/or harmonic phonons at multiple pressures and use those to evaluate the free energy as a function of temperature, but those are not considered here. Repeated phonon calculations in particular would require computational effort comparable to that of the quasi-harmonic approach.

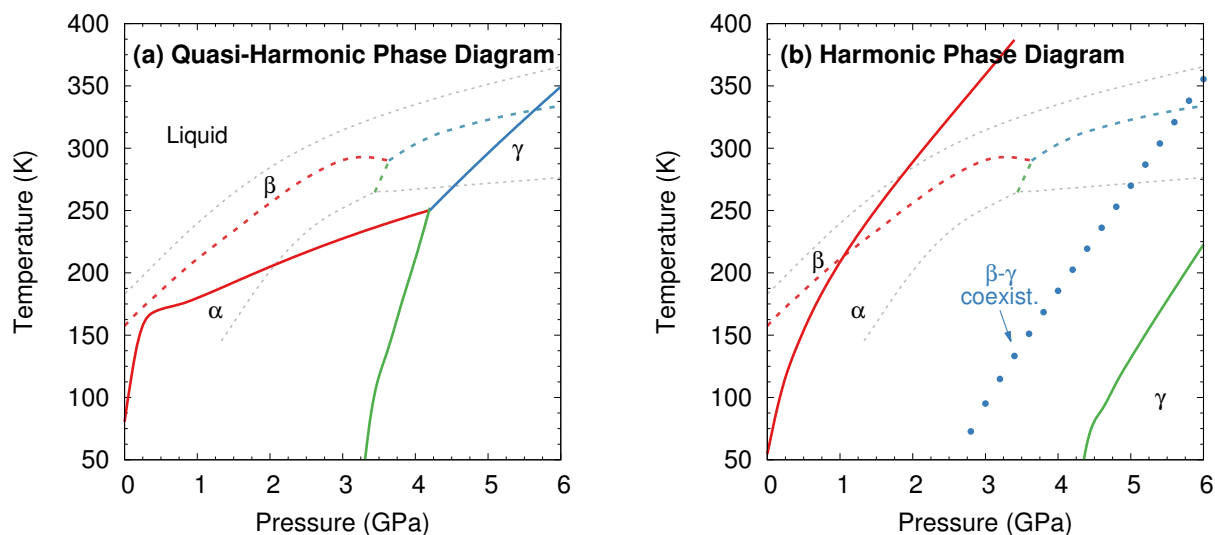


**Figure S7:** Comparison of predicted CCSD(T)/CBS + periodic HF phase diagrams with (a) quasi-harmonic (identical to Figure 2b in the main paper) and (b) harmonic treatments of the phonons. The dotted blue line in the harmonic phase diagram indicates where the  $\beta$ - $\gamma$  coexistence curve would occur, but the  $\alpha$  polymorph is thermodynamically favored in that temperature/pressure regime.

## S5.2 Impact of electron-electron correlation treatment

One might also consider using a lower-level electronic structure methods for the quantum mechanical monomers and dimers in HMBI. As discussed in Section S2 and shown in Figure S8a, MP2/CBS generates  $E(V)$  curves that are very similar to those from CCSD(T)/CBS. That is unsurprising, since MP2 generally performs well for hydrogen bonded systems like methanol which do not exhibit strong van der Waals dispersion interactions. However, in the smaller aug-cc-pVTZ basis, MP2 predicts  $\beta$  to be more stable and shifts its electronic energy minimum to a larger cell volume. See also our earlier work on  $\alpha$  methanol<sup>4</sup> and other crystals for more details on how basis set impacts molar volume and other crystal properties.<sup>16-18</sup>

Figure S8b shows how these variations impact the predicted  $\alpha$ - $\beta$  coexistence curve. In the CBS limit, MP2 and CCSD(T) predict a largely similar phase coexistence curve, though details such as the temperature of the ambient pressure phase transition differ appreciably. Interestingly, the prominent “bump” in the MP2/CBS coexistence curve near 0.5 GPa arises from the seemingly subtle differences between the MP2/CBS and CCSD(T)/CBS energy curves. In contrast to the complete basis set results, MP2/aug-cc-pVTZ erroneously predicts that at ambient pressure the  $\beta$  phase will always be thermodynamically more stable than the  $\alpha$  form at pressures below  $\sim 0.7$  GPa. This data highlights the importance of using electronic structure results that are well-converged with respect to the electron correlation and basis set.

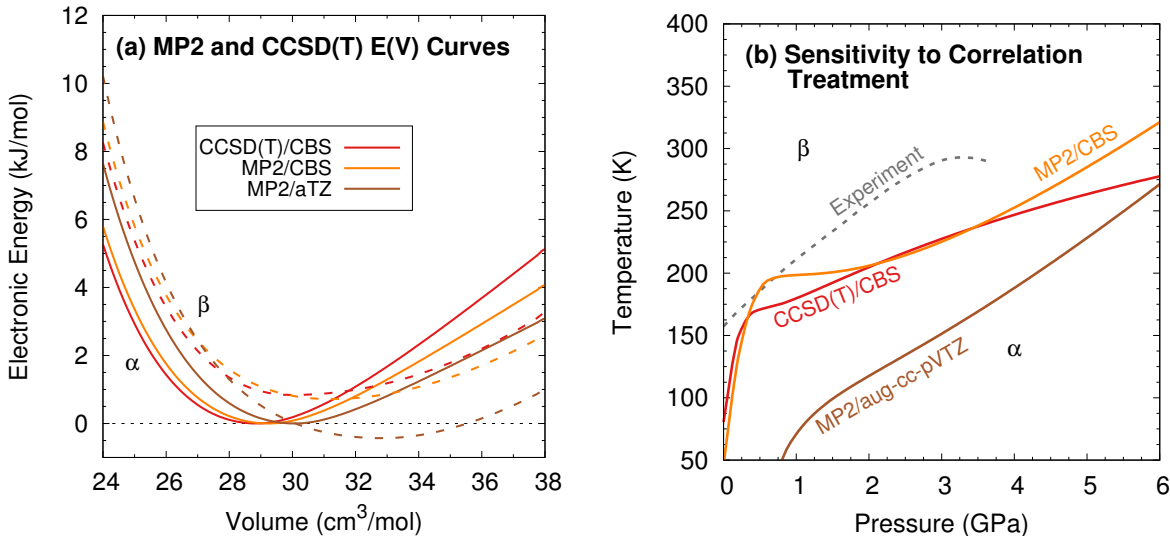


**Figure S8:** Impact of electronic structure method on (a) the  $E(V)$  curves, with the  $\beta$  curves (dotted lines) plotted relative to the minimum energy on the corresponding  $\alpha$  curve (solid lines) and (b) the resulting  $\alpha$ - $\beta$  coexistence curve at the same three levels of theory. Periodic HF many-body contributions were used in all cases.

### S5.3 Impact of electronic energy well steepness

Changing basis set and the treatment of electron-electron correlation as in Section S5.2 impacts both the relative energies of the different polymorphs as well as the shape of the potential energy wells. To help disentangle these effects, we scale just the steepness of the compression and expansion branches of the electronic energy wells. This is done by multiplying the  $\alpha$  and/or  $\beta$  wells by  $\pm 5\%$  (with each well minimum set to 0 kJ/mol for scaling purposes). The resulting  $\alpha$ - $\beta$  phase boundaries were predicted and plotted in Figure S9a. Scaling a well by 0.95 softens the expansion and compression branch, which in turn increases the thermal expansivity and compressibility. Scaling  $E(V)$  by 1.05 has the opposite effect. The change in volume induced by scaling the well will also impact the size of the  $A_{vib}$  contribution, which is smaller at larger volumes (Figure S3).

Because different electronic structure models might impact the  $\alpha$  and  $\beta$   $E(V)$  curves differently, Figure S9 considers different possible scaling combinations. The largest impacts on the  $\alpha$ - $\beta$  coexistence curve from scaling the energy wells occurs at higher pressures and temperatures, where the energy changes are most significant. Either increasing the steepness of the  $\beta$  well or softening the  $\alpha$  potential raises the temperature of the  $\alpha$ - $\beta$  phase coexistence curve at higher pressures. Increasing the  $\alpha$  curve steepness and/or softening the  $\beta$  curve has the opposite effect, lowering the transition temperature appreciably. On the other hand, scaling the two curves in the same direction (both steeper or both softer) has relatively little impact on the potential. As for the MP2 vs CCSD(T) results above, the minor perturbations to  $E(V)$  here impact the presence of the ‘‘bump’’ in coexistence curve near 0.5 GPa. Overall, the results in Figure S9 indicate that errors in the slope of the  $\alpha$ - $\beta$  phase coexistence curve can result from subtle errors in the steepness of the potential energy curves.

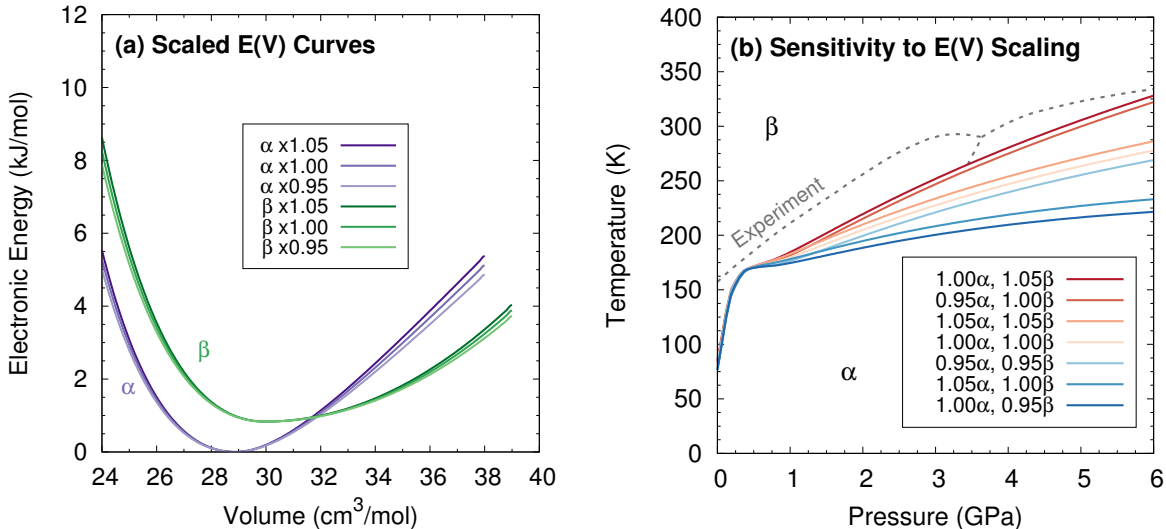


**Figure S9:** (a) Scaling the steepness of the  $\alpha$  and  $\beta$  CCSD(T)/CBS + periodic HF electronic energy wells by only  $\pm 5\%$  (b) significantly impacts the slope of the predicted  $\alpha$ - $\beta$  coexistence curve.

## S5.4 Impact of phonon frequency scaling

Harmonic phonons provide the input frequencies for the quasi-harmonic model. It is well known that harmonic frequencies overestimate the observed vibrational frequencies. Our previous study<sup>4</sup> compared the predicted and experimental phonons for  $\alpha$  methanol and considered several possible empirical scaling approaches that might improve agreement between the predicted and experimental frequencies. One approach is to minimize the difference between the calculated and observed frequencies by scaling all frequencies to by 0.92. Alternatively, one might fit separate scale factors to frequencies within different sub-domains of the phonon spectrum: 0.9302 for high frequencies (above 2000  $\text{cm}^{-1}$ ), 0.9682 for low-frequency intramolecular modes (below 2000  $\text{cm}^{-1}$ ), and values ranging 0.6–0.8 for the lattice phonons. Because the lattice phonon assignments are more ambiguous, we simply explored several different scaling factors in the 0.6–0.8 range to understand the range of possible outcomes. See Ref 4 for details.

Scaling the frequencies in this manner decreases the magnitude of the zero-point energy and makes the slope of the Helmholtz vibrational free energy  $A_{vib}$  versus volume slightly steeper (Figure S10a–b). The zero-point contribution dominates here and leads to a modest contraction in the molar volumes (See Figure 8 in Ref 4). However, because the frequencies for both polymorphs are scaled identically, the changes largely cancel in the vibrational free energy difference between the  $\alpha$  and  $\beta$  forms (Figure S10c). This translates to frequency scaling having only a small impact on the predicted  $\alpha$ - $\beta$  coexistence curve (Figure S10d), in marked contrast to the other variables.

On the other hand, non-uniform errors in the phonon frequencies between the polymorphs could have a larger impact on the predicted phase boundaries. As shown in Figure S11, if one scales only the  $\beta$  phase phonons by 0.5% or 1%, the phase transition boundaries move considerably. The slopes of the  $\beta$  form Helmholtz vibrational free energy curves in Figure S11a are nearly identical with different scalings, but they are offset by the difference in zero-point vibrational energy. The  $\pm 0.5\%$  scaling alters the zero-point energy by 0.7 kJ/mol, effectively shifting the relative stabilities of the two energy wells akin to Figure 4 in the main article.

As noted in the main paper, the calculations underestimate the experimental heat capacity (Figure 3). Earlier analysis on the  $\alpha$  polymorph<sup>4</sup> indicated that underestimation of the heat capacity at temperatures below  $\sim 60$  K likely stems from overestimation of the lattice mode phonon frequencies. The underestimation of the thermal expansivity contributes to this problem. At higher temperatures, the neglected anharmonicity in the higher-frequency modes, particularly the methyl rotations, probably becomes more significant. Because the heat capacity is underestimated in both the  $\alpha$  and  $\beta$  phases, some of the resulting error in the predicted  $\alpha$ - $\beta$  enthalpy difference will cancel. Nevertheless, the residual impact of the heat capacity errors on the phase diagram can be inferred from the sensitivity to phonon scaling discussed here.

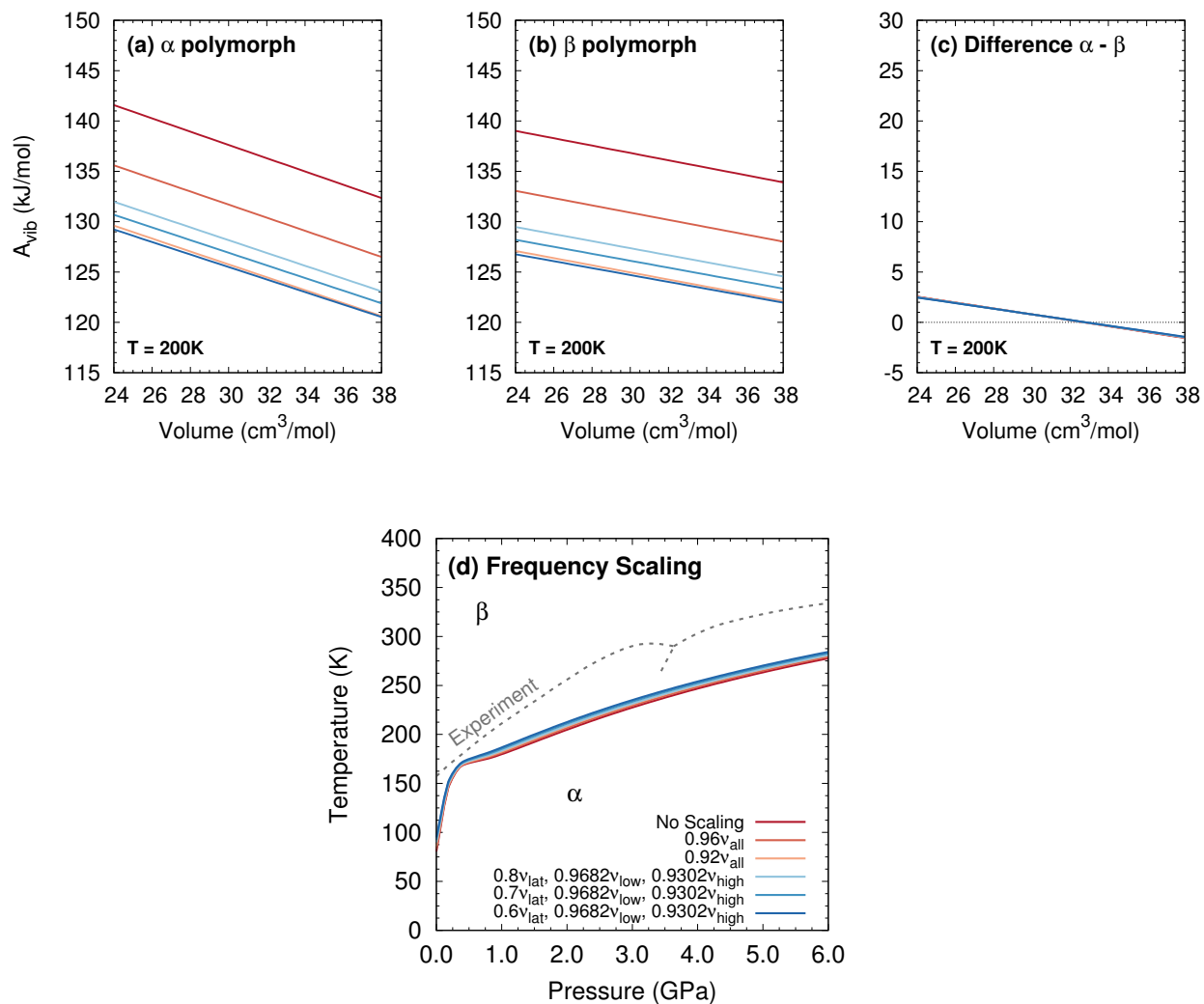


**Figure S10:** Impact of scaling the phonon frequencies on (a) the Helmholtz vibrational free energy of the  $\alpha$  polymorph at 200 K, (b) the Helmholtz vibrational free energy of the  $\beta$  polymorph at 200 K, (c) the difference between the  $\alpha$  and  $\beta$  vibrational free energies, and (d) the predicted  $\alpha$ - $\beta$  coexistence curve. See text for description of the frequency scaling models.

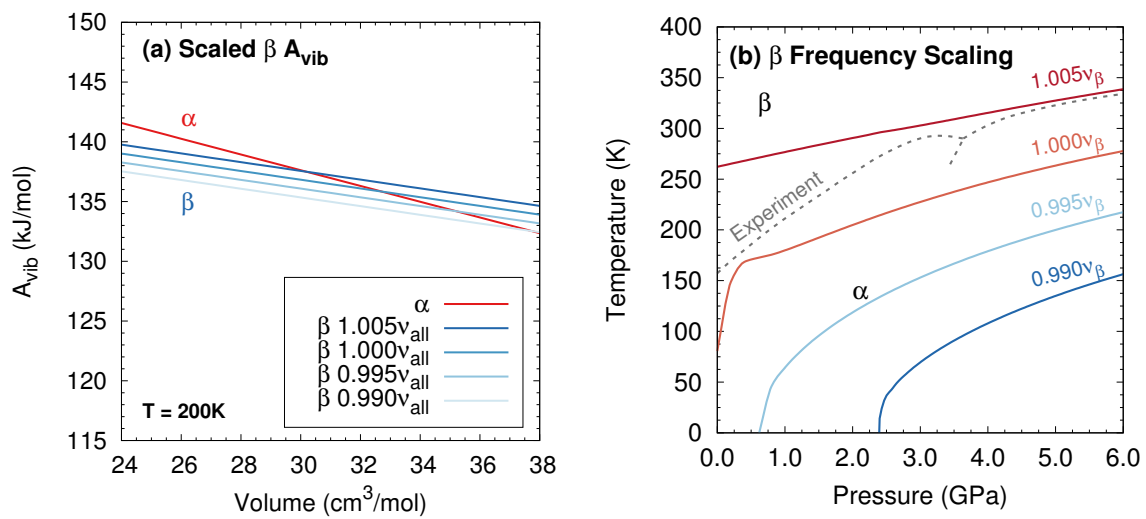


**Figure S11:** Impact of scaling only the  $\beta$  polymorph phonon frequencies on (a) the Helmholtz vibrational free energies at 200 K, and (b) the resulting  $\alpha$ - $\beta$  coexistence curves.

## S5.5 Sensitivity analysis summary

Overall, the sensitivity analysis suggests that the error in the predicted  $\alpha$ - $\beta$  phase transition temperature at ambient pressure can largely be attributed to small ( $\sim 0.5$  kJ/mol) errors in the relative energies of the two phases, while errors in the slopes of the coexistence curve probably stem more from errors in the curvature of the electronic energy wells. The relative stabilities of the minima and the curvature of the electronic energy expansion and compression branches for each phase are sensitive to the electronic structure method used and the zero point vibrational energy. In contrast, the predicted phase diagram appears less sensitive to the thermal contribution from the phonons and/or consistent errors between phases (e.g. scaling the harmonic phonons to approximate anharmonicity). The latter result suggests it might be possible to reduce the computational costs in the future by employing more approximate phonon treatments.

## S6 Does the hypothetical $\delta'$ structure account for the experimental $\delta$ phase?

As discussed in the main paper,  $\gamma$  polymorph is not stable on the electronic energy surface without significant external pressure. Closer investigation of the structure obtained from optimizing the  $\gamma$  form at atmospheric pressure indicates that it is triclinic and overlays very well with the candidate  $\delta'$  structure suggested by Lin et al,<sup>19</sup> especially if the structure obtained here structure is then refined under external pressure 4.5 GPa. Both HMBI and periodic PBE-D3 calculations also identify this structure as a stationary point on the potential energy surface with all real phonon frequencies.

However, preliminary<sup>‡</sup> comparison of Gibbs free energy calculations at the CCSD(T)/CBS + AMOEBA level suggest that this  $\delta'$  polymorph is energetically less stable than the other three methanol polymorphs in the range of thermodynamic conditions considered here. The  $\delta'$  form lies 1.7 kJ/mol above  $\alpha$  at absolute zero and ambient pressure, and increasing temperature or pressure destabilizes  $\delta'$  further relative to  $\alpha$ . While this temperature trend for  $\delta'$  agrees qualitatively with experiment, the pressure dependence is incorrect—the experimental  $\delta$  phase becomes *more stable* at higher pressures, not less. The large molar volume of the  $\delta'$  structure relative to the other phases leads to this incorrect pressure-dependent behavior.

With regard to the  $\gamma$  phase,  $\delta'$  is 3.5 kJ/mol less stable at 4 GPa and 0 K. The  $\delta'$  structure is further destabilized by increasing pressure and temperature (both contrary to the behavior of the experimental  $\delta$  phase). Test calculations replacing the AMOEBA many-body contribution with one from periodic HF reduces the 0 K cohesive energy difference between  $\gamma$  and  $\delta'$  from 3.5 kJ/mol to 2.5 kJ/mol, but this change is insufficient to make the  $\delta'$  structure thermodynamically preferred.

Together, this evidence suggests that the  $\delta'$  phase is not likely to account for the experimentally observed  $\delta$  phase. Nevertheless, the  $\delta'$  structure does appear to be dynamically stable (it exhibits all real phonon frequencies), so it might reflect an as yet experimentally unknown thermodynamically metastable polymorph.

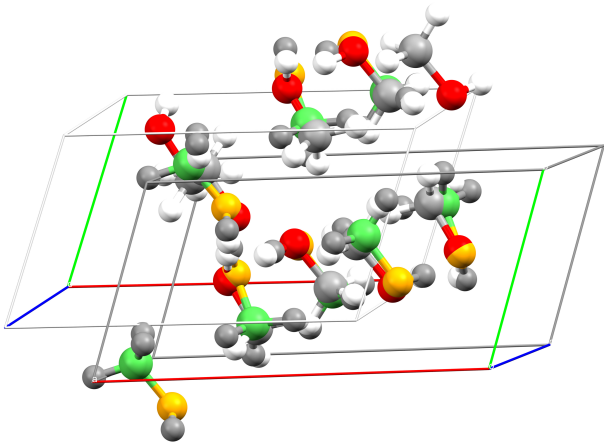


**Figure S12:** Overlay between the DFT  $\delta'$  structure from Ref 19 and the one optimized here, both at 0 K and 4.5 GPa. Lin et al: O=red, C=gray, H=white. This work: O=gold, C=green, H=gray.

<sup>‡</sup>The preliminary  $\delta'$  calculations approximated  $E(V)$  from constant-volume isotropic calculations, instead of anisotropic constant-pressure ones, and included only two CCSD(T)/CBS single-point energies. This was sufficient to show that the  $\delta'$  structure is less stable than the others and that it will not be preferred at the thermodynamic conditions where the  $\delta$  phase exists experimentally.

## References

- (1) Würflinger, A.; Landau, R. Differential thermal analysis at high pressures—VII: Phase behaviour of solid methanol up to 3 kbar. *J. Phys. Chem. Solids* **1977**, *38*, 811–814.
- (2) Gromnitskaya, E. L.; Stal’gorova, O. V.; Yagafarov, O. F.; Brazhkin, V. V.; Lyapin, A. G.; Popova, S. V. Ultrasonic study of the phase diagram of methanol. *J. Expt. Theor. Phys. Lett.* **2004**, *80*, 597–601.
- (3) Kondrin, M. V.; Pronin, A. A.; Lebed, Y. B.; Brazhkin, V. V. Phase transformations in methanol at high pressure measured by dielectric spectroscopy technique. *J. Chem. Phys.* **2013**, *139*, 084510.
- (4) Červinka, C.; Beran, G. J. O. Ab initio thermodynamic properties and their uncertainties for crystalline  $\alpha$ -methanol. *Phys. Chem. Chem. Phys.* **2017**, *19*, 29940–29953.
- (5) Peintinger, M. F.; Oliveira, D. V.; Bredow, T. Consistent Gaussian basis sets of triple-zeta valence with polarization quality for solid-state calculations. *J. Comp. Chem.* **2013**, *34*, 451–459.
- (6) Müller, C.; Paulus, B. Wavefunction-based electron correlation methods for solids. *Phys. Chem. Chem. Phys.* **2012**, *14*, 7605–7614.
- (7) Beran, G. J. O. Modeling polymorphic molecular crystals with electronic structure theory. *Chem. Rev.* **2016**, *116*, 5567–5613.
- (8) Staveley, L. A. K.; Hogg, M. A. P. A dilatometric study of the transition in methyl alcohol. *J. Chem. Soc.* **1954**, 1013–1016.
- (9) Nagayoshi, K.; Kitaura, K.; Koseki, S.; Re, S.; Kobayashi, K.; Choe, Y.-K.; Nagase, S. Calculation of packing structure of methanol solid using ab initio lattice energy at the MP2 level. *Chem. Phys. Lett.* **2003**, *369*, 597–604.
- (10) Červinka, C.; Fulem, M.; Růžička, K. CCSD(T)/CBS fragment-based calculations of lattice energy of molecular crystals. *J. Chem. Phys.* **2016**, *144*, 064505.
- (11) Ren, P.; Wu, C.; Ponder, J. W. Polarizable Atomic Multipole-based Molecular Mechanics for Organic Molecules. *J. Chem. Theory Comput.* **2011**, *7*, 3143–3161.
- (12) Červinka, C.; Fulem, M. State-of-The-Art Calculations of Sublimation Enthalpies for Selected Molecular Crystals and Their Computational Uncertainty. *J. Chem. Theory Comput.* **2017**, *13*, 2840–2850.
- (13) Reilly, A. M.; Cooper, R. I.; Adjiman, C. S.; Bhattacharya, S.; Boese, A. D.; Brandenburg, J. G.; Bygrave, P. J.; Bylisma, R.; Campbell, J. E.; Car, R.; Case, D. H.; Chadha, R.; Cole, J. C.; Cosburn, K.; Cuppen, H. M.; Curtis, F.; Day, G. M.; DiStasio Jr, R. A.; Dzyabchenko, A.; van Eijck, B. P.; Elking, D. M.; van den Ende, J. A.; Facelli, J. C.; Ferraro, M. B.; Fusti-Molnar, L.; Gatsiou, C.-A.; Gee, T. S.; de Gelder, R.;

- Ghiringhelli, L. M.; Goto, H.; Grimme, S.; Guo, R.; Hofmann, D. W. M.; Hoja, J.; Hylton, R. K.; Iuzzolino, L.; Jankiewicz, W.; de Jong, D. T.; Kendrick, J.; de Klerk, N. J. J.; Ko, H.-Y.; Kuleshova, L. N.; Li, X.; Lohani, S.; Leusen, F. J. J.; Lund, A. M.; Lv, J.; Ma, Y.; Marom, N.; Masunov, A. E.; McCabe, P.; McMahon, D. P.; Meekes, H.; Metz, M. P.; Misquitta, A. J.; Mohamed, S.; Monserrat, B.; Needs, R. J.; Neumann, M. A.; Nyman, J.; Obata, S.; Oberhofer, H.; Oganov, A. R.; Orendt, A. M.; Pagola, G. I.; Pantelides, C. C.; Pickard, C. J.; Podeszwa, R.; Price, L. S.; Price, S. L.; Pulido, A.; Read, M. G.; Reuter, K.; Schneider, E.; Schober, C.; Shields, G. P.; Singh, P.; Sugden, I. J.; Szalewicz, K.; Taylor, C. R.; Tkatchenko, A.; Tuckerman, M. E.; Vacarro, F.; Vasileiadis, M.; Vazquez-Mayagoitia, A.; Vogt, L.; Wang, Y.; Watson, R. E.; de Wijs, G. A.; Yang, J.; Zhu, Q.; Groom, C. R. Report on the sixth blind test of organic crystal structure prediction methods. *Acta Cryst. B* **2016**, *72*, 439–459.
- (14) Nyman, J.; Day, G. M. Static and lattice vibrational energy differences between polymorphs. *CrystEngComm* **2015**, *17*, 5154–5165.
- (15) Nyman, J.; Day, G. M. Modelling temperature-dependent properties of polymorphic organic molecular crystals. *Phys. Chem. Chem. Phys.* **2016**, *18*, 31132–31143.
- (16) Heit, Y. N.; Nanda, K. D.; Beran, G. J. O. Predicting finite-temperature properties of crystalline carbon dioxide from first principles with quantitative accuracy. *Chem. Sci.* **2016**, *7*, 246–255.
- (17) Heit, Y. N.; Beran, G. J. O. How important is thermal expansion for predicting molecular crystal structures and thermochemistry at finite temperatures? *Acta Cryst. B* **2016**, *72*, 514–529.
- (18) McKinley, J. L.; Beran, G. J. O. Identifying pragmatic quasi-harmonic electronic structure approaches for modeling molecular crystal thermal expansion. *Faraday Disc.* **2018**, *in press*.
- (19) Lin, T.-J.; Hsing, C.-R.; Wei, C.-M.; Kuo, J.-L. Structure prediction of the solid forms of methanol: an ab initio random structure searching approach. *Phys. Chem. Chem. Phys.* **2016**, *18*, 2736–2746.